Monitoring greenhouses gases over China using space−based observations

BOESCH H.[1,2], LIU Y[3], PALMER P I [4,5], TAMMINEN J[6], ANAND J[1,2], CAI Z[3], CHE K[3], CHEN H[7], CHEN X[3], FENG L[4,5], HAKKARAINEN J[6], HEIKKINEN P[6], KALAITZI N[1,2], KIVI R[6], PARKER R[1,2], SOMKUTI P[1,2], WANG J[3], WEBB A[1,2], YANG D[3], YAO L[3], YI Y[3],

1. *Department of Physics, Astronomy, University of Leicester, Leicester, UK;*
2. *National Centre for Earth Observation NCEO, University of Leicester, UK;*
3. *Key Laboratory of the Middle Atmosphere and Global Environmental Observation, Institute of Atmospheric Physics, Chinese Academy of Sciences, Beijing, China;*
4. *School of GeoSciences, University of Edinburgh, Edinburgh, UK;*
5. *National Centre for Earth Observation NCEO, University of Edinburgh, UK;*
6. *Finnish Meteorological Institute, Helsinki, Finland;*
7. *Groningen University, Groningen, Netherlands*

Abstract: The atmospheric carbon dioxide (CO_2) concentration has increased to more than 405 parts per million (ppm) in 2017 due to human activities such as deforestation, land-use change and burning of fossil fuels. Although there is broad scientific consensus on the damaging consequences of the change in climate associated with increasing concentrations of greenhouse gases, fossil CO_2 emissions have continued to increase in recent years mainly from rapidly developing economies and China is now the largest emitter of CO_2 generating about 30% of all emissions globally. To allow more reliable forecast of the future state of the carbon cycle and to support the efforts for mitigation greenhouse gas emissions, a better understanding of the global and regional carbon budget is needed. Space-based measurements of CO_2 can provide the necessary observations with dense coverage and sampling to provide improved constrains on of carbon fluxes and emissions. The Chinese Global Carbon Dioxide Monitoring Scientific Experimental Satellite (TanSat) was established by the National High Technology Research and Development Program of China with the main objective of monitoring atmospheric CO_2 and CO_2 fluxes at the regional and global scale. TanSat has been successfully launched in December 2016 and as part of the Dragon programme of ESA and the Ministry of Science and Technology (MOST), a team of researchers from Europe (UK and Finland) and China has evaluated early TanSat data and contrast it against data from the GOSAT mission and models. In this manuscript, we report on retrieval intercomparisons of TanSat data using two different retrieval algorithms, on validation efforts for the Eastern Asia region using GOSAT CO_2 data and first assessments of TanSat and GOSAT CO_2 data against model calculations using the GEOS-Chem model.

Key words: carbon cycle; spectroscopy; satellite remote sensing

Citation format: Boesch H,Liu Y,Palmer P I,Tamminen J,Anand J,Cai Z,Che K,Chen H,Chen X,Feng L,Hakkarainen J, Heikkinen P, Kalaitzi N, Kivi R, Parker R, Somkuti P, Wang J, Webb A, Yang D, Yao L and Yi Y. 2020. Monitoring greenhouses gases over China using space−based observations. Journal of Remote Sensing(Chinese). 24(S1): 58−65

1 INTRODUCTION

The atmospheric carbon dioxide (CO_2) concentration has increased by more than 46% since the beginning of the industrial revolution to more than 405 parts per million (ppm) in 2017 (Le Quere, et al., 2018) due to deforestation and land-use change, cement production and extraction and burning of fossil fuels. The latter has become the dominant source since the 1950's and fossil-fuel emissions are now contributing 87% of global emissions. CO_2 is a strong greenhouse gas and its increased concentrations alter the Earth's radiative equilibrium contributing over 1.82 W/m^2 additional radiative forcing as of 2011. Together with additional contributions from methane, nitrous oxide and other greenhouse gases, this has resulted in an increase in global temperature of 0.85 °C (IPCC, 2013). Although there is broad scientific consensus on the damaging consequences of further increasing global temperatures and the associated climate change, the causative fossil CO_2 emissions have continued to increase, and in 2014, they were 55% above the levels of 1990. This continued acceleration of emissions is mainly linked to rapidly developing economies with developing nations contributing 60% of the global emissions in 2013 compared to 32% in 1990. China has now become the largest emitter of CO_2 generating about

Received: XXXX-XX-XX; **Accepted:** XXXX-XX-XX

30% of all emissions which highlights the need for a better understanding of the carbon budget for this key region.

Measurements of atmospheric CO_2 from space can provide global coverage with high spatial and temporal coverage which will be a key step towards improvements in our understanding of carbon fluxes and emissions, in particularly for regions poorly sampled by surface networks. Measurements in the near infrared (NIR) and shortwave infrared (SWIR) spectral region appear best suited as they can provide sufficient precision and high sensitivity to the boundary layer where the effect of sources and sinks is largest. The first satellite to measure atmospheric CO_2 column-averaged dry air mole fractions (XCO_2) from the NIR/SWIR was the Scanning Imaging Absorption Spectrometer for Atmospheric Chartography (SCIAMACHY) onboard ESA ENVISAT (Bovensmann et al, 1999) launched in 2002. In 2009, the Japanese Greenhouse Observing Satellite (GOSAT, Kuze, et al., 2009) instrument; the first dedicated greenhouse gas monitoring satellite was launched followed by NASA's Orbiting Carbon Observatory 2 (OCO-2) in July 2014 (Crisp, et al., 2017).

As the largest developing country, China faces a serious problem of greenhouse gas (GHG) emissions. To pursue sustainable development and reduce GHG emissions, better quantification of the carbon budget at regional scales is critical and has become a significant focus. The Chinese Global Carbon Dioxide Monitoring Scientific Experimental Satellite (TanSat) was established by the National High Technology Research and Development Program of China (863 Program) with the main objective to monitor the XCO_2 and CO_2 flux at the regional and global scale (Li, et al., 2017).

TanSat was launched successfully in December 2016 after 6 years of development, and completed its on-orbit tests and calibration in 2017. It aims to measure XCO_2 with a precision of better than 4 ppm at regional scale in order to provide data needed to constrain global and regional CO_2 fluxes. There are two instruments on-board TanSat. The Atmospheric Carbon Dioxide Grating Spectrometer (ACGS) is the main instrument and is a hyperspectral instrument that is designed to measure NIR/SWIR backscattered sunlight in the molecular oxygen (O_2) A-band (0.76 μm) and two CO_2 bands (1.61 and 2.06 μm). The key parameters are listed in Table 1. In addition, to better correct the effects from aerosols and cirrus clouds (Zhang et al, 2013), there is a co-located instrument onboard TanSat, Cloud and Aerosol Polarization Imager (CAPI). CAPI is a wide field of view (FOV) moderate resolution imaging spectrometer that can simultaneously measure radiances in five atmospheric window bands (380, 670, 870, 1375,and 1640 nm) as well as polarization in a visible band (670 nm) and a near infrared band (1640 nm) which is used to achieve more information on aerosol size distribution. In fact, a channel centered at 1375 nm is employed for improving screening for cirrus.

The TanSat has three observation modes in operation, including nadir, sun-glint and target mode. Nadir mode is the common observation mode that is active over land with tracking the principle plan to avoid effects from the reflectance of Brewster's angle and guarantee that the polarization conditions are identical throughout the flight. The ocean surface is very dark in nadir and hence, the Signal to Noise Ratio (SNR) is relatively low. In order to improve the measurement quality, the satellite observes the sun glint over the ocean surface with the instrument boresight point located within five degrees of the principal plane. In order to investigate the emission of hot spots, the satellite has the capability in target mode to focus on a small area and observe this continuously with different view angles (-60° to 60°). It also can be used to observe CO_2 validation stations on the ground in order to validate the quality of the measurement.

Table 1 Specifications of key characteristics of Carbon Dioxide Sensors

	O_2–A	CO_2 Weak	CO_2 Strong
Spectral Range /nm	758 – 778	1594 – 1624	2042 – 2082
Spectral Resolution /nm	0.039 – 0.042	0.123 – 0.128	0.16 – 0.17
Signal to Noise Ratio (SNR)	455@0.0152W m^{-2} sr^{-1} nm^{-1}	260@0.0026 W m^{-2} sr^{-1} nm^{-1}	185@0.0011 W m^{-2} sr^{-1} nm^{-1}
Spatial Resolution /km	2 × 2		
Swath /km	18		

Notes: Mean SNR through all pixels.

In this manuscript, we report on the efforts of a collaboration between European (UK and Finland) and Chinese teams under the framework of the Dragon programme of ESA and the Ministry of Science and Technology (MOST) to evaluate the early results from the TanSat mission in conjunction with observations from GOSAT. The focus is on characterisation of the performance of current retrieval methods by retrieval intercomparisons (section 2), to assess the performance of CO_2 satellite data over China and the wider region based on ground-based validation data (section 3), and to evaluate satellite CO_2 observations from GOSAT and TanSat against calculations from atmospheric transport models and to assess the capability of current satellite missions to observe emission patterns (section 4).

2 SATELLITE RETRIEVAL METHODS

The back-scattered sunlight in the NIR/SWIR range as measured by satellites is influenced by absorption from gases, scattering by aerosols and clouds and reflection from the surface which leads to a complicated radiative transfer problem which requires the use of complex Full Physics (FP) retrieval algorithms.

The IAPCAS algorithm involves a highly accurate radiative transfer model (RTM) to simulate the spectral measurements taking into account the interference from the atmosphere and surface. By comparing observed and simulated spectra, a number of atmospheric and surface variables are inferred simultaneously (the so-called state vector), including a profile of atmospheric CO_2 concentrations. TanSat tracks the principle plane inflight and a polarizer in front of the collimator only transmits light into instrument parallel to the slit. Thus, the algorithm employs the vector linearized discrete ordinate radiative transfer model (VLIDORT) to compute Stokes parameters to describe the polarized light that the instrument measures. The retrieval algorithm uses atmospheric profiles given on twenty equidistant pressure intervals. Each interval is subdivided into ten sub-layers for the calculation of the optical properties which allows the reduction of errors in the absorption cross-sections from non-linearities in pressure and temperature. Correct treatment of the surface reflectance is important for the radiative transfer which requires complicated functions that depend on the

incident and emergent angle. Here, we use the simplification of a Lambertian surface because of a lack of information in the observed spectrum on the parameters in a surface model and because the radiance in emergent direction is by far the most important direction. Besides aerosol information from CAPI measurements, aerosol information can also be obtained from the ACGS hyperspectral observations. As shown in Chen, et al. (2018, under review), only four to seven pieces of independent aerosol information can be retrieved from ACGS hyperspectral observations for aerosols. After comparing the components of XCO_2 retrieval error induced by aerosol uncertainties, one aerosol model including seven parameters is recommended in the CO_2 retrieval to minimize the aerosol interference as studied in Chen, et al. (2018, under review). The O_2 A band provides information on surface pressure and on the light path modification not only aerosol but also cloud and surface elevation. However, the wavelength dependence of aerosol extinction across the NIR/SWIR is significant. Therefore, the aerosol information from the O_2 A band is not well representing the CO_2 bands, and variations exist even between CO_2 bands. The Ångström exponent, α, is a well-established concept to describe this wavelength dependence of aerosol extinction. Sensitive studies on the Ångström exponent for typical aerosols indicate that the wavelength dependence is not well described by a simple Ångström exponent. Therefore, in IAPCAS, we extend the Ångström exponent to a quadratic form and retrieve the mode radius of aerosol particles to constrain this wavelength dependence. In addition, aerosol total column and vertical distribution are important, and hence AOD, aerosol layer centre height and width (normal distribution of AOD assumption) are retrieved. The IAPCAS algorithm adopts the well-known Optimal Estimation Method (OME) (Rodgers, 2000), to find the maximum posteriori probability for the state vector by minimizing a cost function. Once the iterative process has successfully converged, XCO_2 can be deduced from the CO_2 profile by applying a pressure-weighted average. The IAPCAS retrieval algorithm has been applied in GOSAT measurement (Liu, et al., 2013; Yang, et al., 2015), referred to as ATANGO (Application of TanSat XCO_2 retrieval algorithm on GOSAT Observation). Preliminary XCO_2 data was produced from Feb. to July 2017 with the IAPCAS algorithm and the first global map of XCO_2 has been generated (Yang, et al., 2017, 2018) and shown at the 2017 GEO meeting in Washington D.C., U.S. The validation results with 8 TCCON (Total Carbon Column Observing Network) stations indicate a 2.11 ppm uncertainty in average (Liu, et al., 2018).

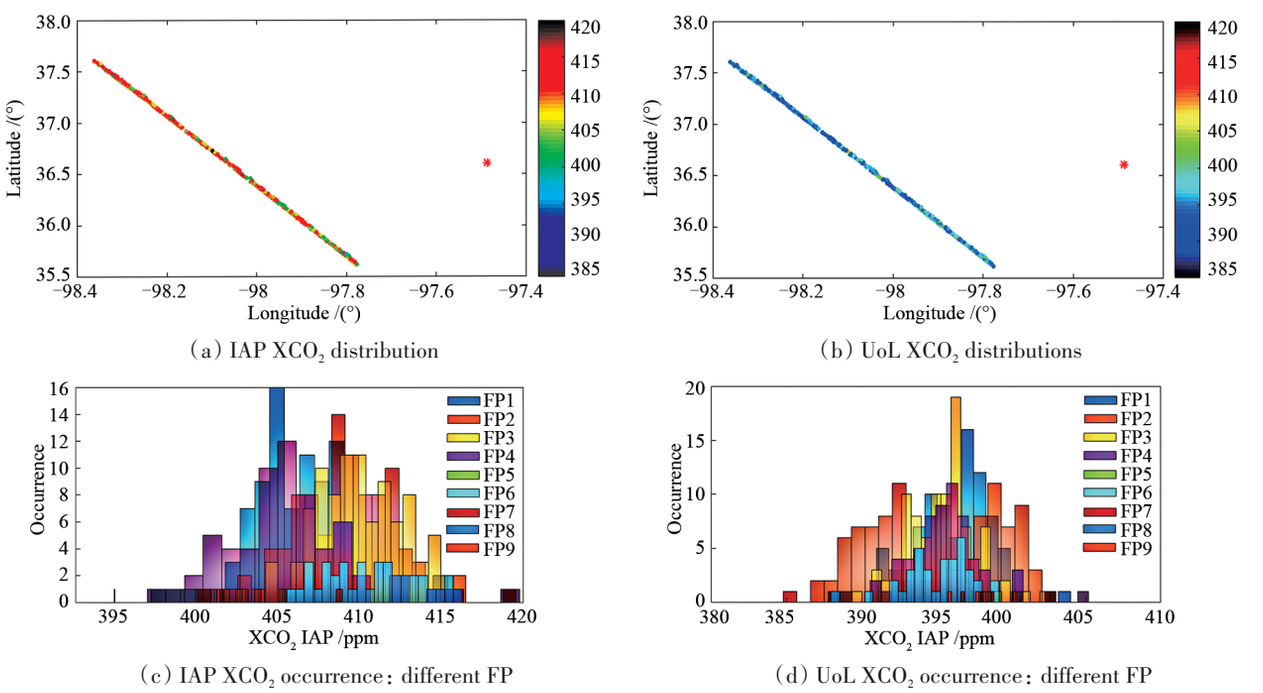

(a) IAP XCO_2 distribution

(b) UoL XCO_2 distributions

(c) IAP XCO_2 occurrence: different FP

(d) UoL XCO_2 occurrence: different FP

Fig.1 The preliminary XCO_2 retrieval intercomparisons for a case study around the Lamont TCCON site on Oct. 8, 2017

Similar to the IAPCAS algorithm, the University of Leicester full physics (UoL-FP) retrieval algorithm is based on a non-linear, iterative retrieval scheme using the Bayesian optimal estimation method of (Boesch, et al., 2011). The Forward model of UoL-FP employs the LIDORT radiative transfer model combined with a fast 2-orders-of-scattering vector radiative transfer code to approximate polarisation, (Natraj, et al., 2008). The code uses the Principal Component Analysis method (PCA) of Somkuti, et al., (2018) to accelerate the radiative transfer component of the retrieval algorithm. The retrieval retrieves profiles of atmospheric variables on 20 levels (including CO_2) together with information on surface reflectance and aerosol parameters. The UoL-FP retrieval retrieves aerosol extinction profiles for two aerosol retrieval types that are created based on aerosol information from the Copernicus Atmospheric Monitoring Service CAMS. In addition, a cirrus profile is included in the retrieval. The UoL algorithm also employs the Levenberg-Marquardt modification of the Gauss-Newton method to find the estimate of the state vector with the maximum a posteriori probability, given the measurement. The UoL-FP algorithm has been used to generate the global CO_2 data from GOSAT for the ESA Climate Change Initiative CCI and the Copernicus Climate Change Service C3S (Buchwitz, et al., 2017).

In order to characterise the CO_2 retrieval from TanSat, an intercomparison between the UoL-FP and IAPCAS retrieval has been carried out for clear-sky measurements over land while TanSat is in its nadir mode. The Aqua/MODIS cloud mask data (MYD35 V6) and RGB image has been used to select cloud-free data. We use the TanSat V2.0 L1B product which has is significantly im-

proved calibration compared to previous versions and we have selected an orbit on 8 Oct. 2017 close to the TCCON station at Lamont, USA, and which has minimal cloud contamination. In addition, to reduce the risk of thin cloud impacts on the retrieval, we applied a O_2 A band cloud screening on the measurement before the CO_2 retrieval. This fast O_2 A band cloud screening algorithm retrieves only apparent surface pressure for assumed clear sky condition. Thus, any modifications to the light path due to scattering will cause the apparent surface pressure to change from the meteorological surface pressure taken from the ECMWF reanalysis product. We have allowed a threshold value of 20 hPa to identify cloud perturbations.

The preliminary XCO_2 results from IAPCAS and UoL-FP are shown in Fig. 1. The mean XCO_2 values from IAPCAS is 408.7 and from UoL-FP is 395.8 ppm respectively, while TCCON measurements show a mean value of 403.5 ppm suggesting an overestimate of 5.23 ppm by IAPCAS and an underestimate of 7.71 ppm by UoL-FP. We also notice the difference between the nine across-track footprints of TanSat as shown in the XCO_2 distribution given as histograms per footprint in Fig. 1. All footprints indicate an approximate normal distribution which is a reflection of the random errors from noise and other uncertainties. The difference between the UoL-FP and IAPCAS and between the footprints is an indication of potential uncertainties in instrument calibration which is expected to improve in future releases of the Level 1b data.

3 VALIDATION APPROACHES

The TCCON network is a global network of ground-based Fourier Transform Spectrometers (FTS) that provides CO_2 columns with accuracies near 0.1% (~0.4 ppm) and is known as the primary network for validating space-based CO_2 observations (Wunch, et al., 2011). To achieve traceability to the ground-based *in situ* standards maintained by the WMO GAW, TCCON XCO_2 is validated against vertical profiles of *in situ* measurements obtained by high-altitude aircraft flights above the stations or by AirCore measurements.

AirCore is an atmospheric sampling system to measure vertical profiles of gases in the troposphere and stratosphere (Karion, et al., 2010). Compared to the aircraft measurements, balloon-borne AirCore has the benefit of also sampling also stratospheric altitudes, thus reducing the uncertainty of column retrievals. AirCore measurements can also be directly used to evaluate satellite borne or ground based FTS retrievals (e.g. Tukiainen, et al., 2016; Wang, et al., 2017). A meteorological balloon (Fig. 2) lift the AirCore system to the stratosphere typically up to about 30-35 km in altitude. The sampler is filled during the descent of the AirCore from the stratosphere down to the surface, making use of the pressure difference between the sampler and the ambient air. A large parachute is attached to the payload to reduce the descent speed of the sampler. We have performed a series of AirCore flights at the Sodankylä TCCON site (Kivi and Heikkinen, 2016) since September 2013. The AirCore system is built as a stainless-steel tubing of about 100 m length. The AirCore configuration makes it possible to measure profiles with vertical resolution of 5 hPa in the stratosphere and 15 hPa in the troposphere. The system measures also ambient pressure, wind profiles, GPS coordinates as well as water vapor and temperature profiles simultaneously measured by Vaisala RS92 radiosonde (Dirksen, et al., 2014), attached to the AirCore payload. A gas analyser (Picarro G2401) has been used at the measurement site to retrieve CO_2, CH_4 and CO profiles shortly after landing of the AirCore. An example of measured AirCore profiles of the dry air mole fraction (DMF) of CO_2, CH_4 and CO is shown in Fig. 3. The figure also provides a comparison with a priori profiles used in the TCCON retrieval. As part of the Dragon-4 program, researchers from CAS have visited the Finnish Meteorological Institute and joined an AirCore inter-comparison campaign at Sodankylä, Finland during summer 2018. Using subsequently two AirCore systems, a validation campaign for TanSat has been carried out in Inner Mongolia, China in 2018 involving also additional ground-based column-instruments (EM27/SUN).

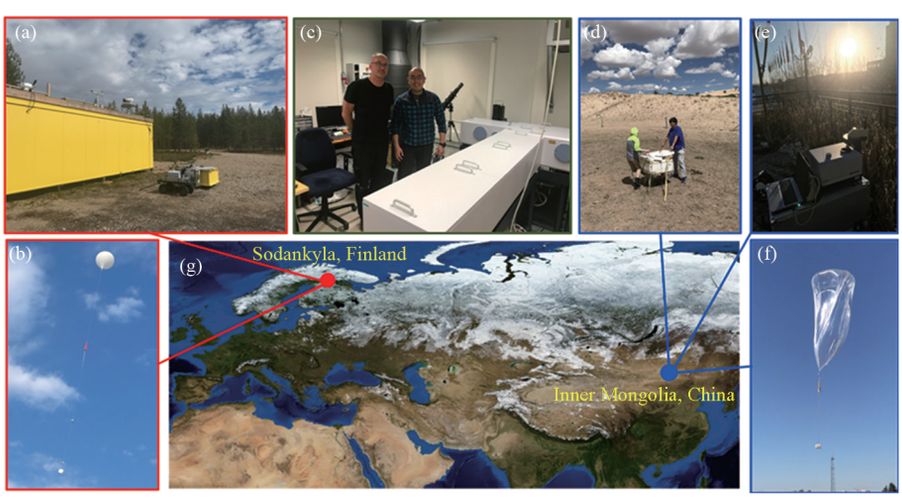

Fig.2 a) ESA FRM4GHG campaign instruments in Sodankylä in June 2018; b) AirCore balloon launch in Sodankyla; c) High-resolution FTS at the Sodankylä TCCON site; d) Field site in Inner Mongolia e) EM27Sun used during the campaign in Inner Mongolia f) AirCore balloon launch in Inner Mongolia g) Map showing the location of the two AirCore sites.

Since 2016, measurements from a TCCON site in China are available (Hefei) and we now have six TCCON sites in Eastern Asia (Goo, et al., 2017, Liu, et al., 2018, Shiomi, et al., 2017, Morino, et al., 2017a, 2017b, 2017c, Oh, et al., 2018, Velazco, et al., 2017) which provides a good opportunity for validating satellite retrievals in this difficult region with high aerosol loading and strong local CO_2 sources. The comparison between these TCCON stations and the UoL-FP GOSAT CO_2 retrieval is shown in Fig. 4. We find

biases between GOSAT and TCCON ranging between -0.98 ppm and 0.69 ppm with a standard deviation (which reflects the scatter of the data) between 1.94 ppm and 2.93 ppm. Although these values are slightly larger than the values found globally for all TCCON sites (Buchwitz, et al., 2017), they are still within expectation and it demonstrates the good performance of the GOSAT retrieval over East Asia.

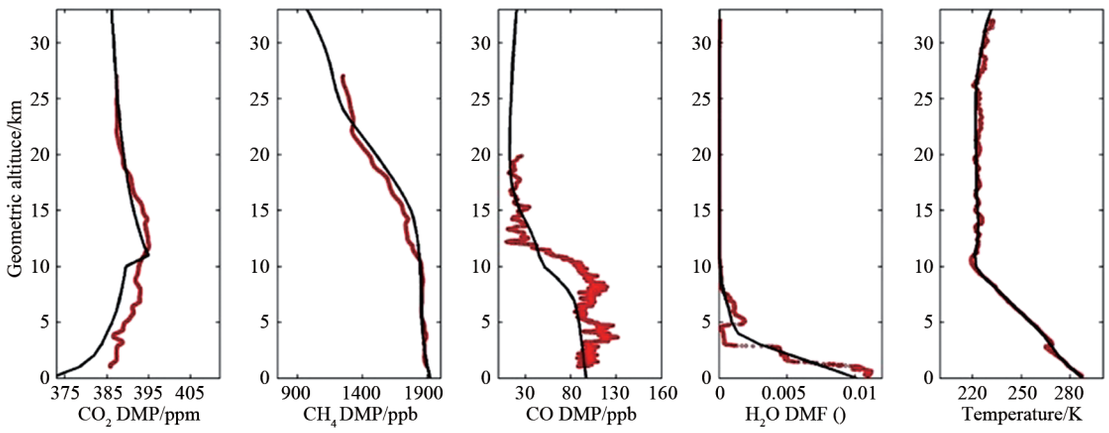

Fig.3 AirCore profiles of the dry air mole fraction (DMF) of CO_2, CH_4 and CO were measured over Sodankylä, Finland in the vicinity of the Sodankylä TCCON site (panels 1–3 from left). Red dots represent the AirCore measurement, while the black line corresponds to the TCCON a priori profile for comparison.

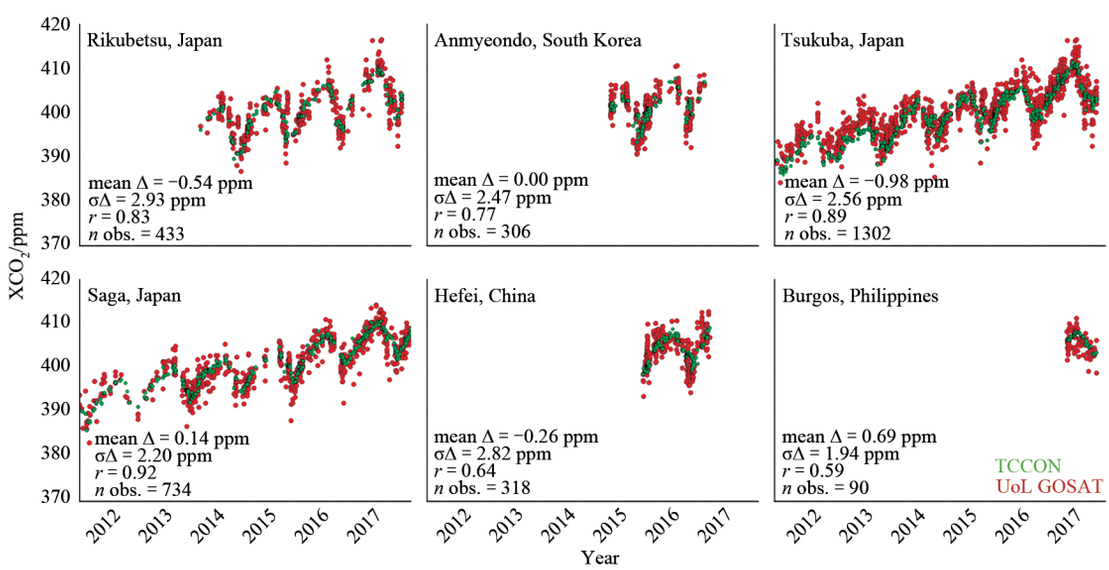

Fig.4 Time series plot of XCO_2 retrieved from GOSAT soundings using the UoL-FP algorithm (red) and co-located TCCON XCO_2 (green) measured from East Asian stations during 2011 – 2018. Co-location of GOSAT and TCCON was performed using the proxy technique developed by Wunch, et al. (2011).

4 MODEL COMPARISONS

The GEOS-Chem model is an offline chemistry transport model (CTM) driven by the GEOS-5 meteorological analyses (GEOS-FP from 2013) from the Global Modelling and Assimilation Office (GMAO) Global Circulation Model based at NASA Goddard Space Flight Center. The model is run with a horizontal resolution of 4° (latitude) ×5° (longitude), using 47 vertical levels from the surface to 0.01 hPa. The atmospheric model simulations are forced by surface fluxes inferred from the ground-based measurements of atmospheric CO_2 concentrations, using an ensemble Kalman Filter (EnKF) framework (Feng, et al., 2009; 2016). In the flux inversion, we use a subset of the global atmospheric surface CO_2 observations network, including discrete (weekly) flask air samples from 105 sites and continuous (hourly) observations from 52 sites. They are chosen from the Observation Package (ObsPack) obspack_co2_1_GLOBALVIEWplus_v3.2_2017_11_02 data product (ObsPack, 2017) from National Oceanic and Atmospheric Administration (NOAA) Earth System Research Laboratory (ESRL). Comparisons of the model simulations are in good agreement with the independent TCCON data, with standard deviation typically smaller than 1.5 ppm.

In Fig. 5, we compare the GOSAT and TanSat XCO_2 retrievals for spring (MAM) 2017 to the model calculations of the GEOS-Chem model. The model is sampled according to the satellite observations. Only cloud-free, quality-filtered data is shown. Both satellite datasets show similar pattern such as the strong North-South gradient in XCO_2 in good agreement with the model data.

Thanks to its denser sampling, a much better coverage is observed for TanSat compared to GOSAT. The difference of the satellite data to the model shows similar patterns for both satellite datasets with a stronger North-South gradient observed in the satellite datasets compared to the model with TanSat showing slightly larger differences to the model. A time series for the region around China (5° — 46° N and 82°—147° E) is given in Fig. 6. The figure shows the GEOS-Chem model and GOSAT XCO_2 data between 2013 and 2018 as well as the TanSat data for the available five months in 2017. Although GOSAT and the model show a similar trend, the model shows a shallower seasonal amplitude which points towards deficiencies in the model in its description of the natural carbon cycle and regional emissions. A similar pattern is observed for the TanSat.

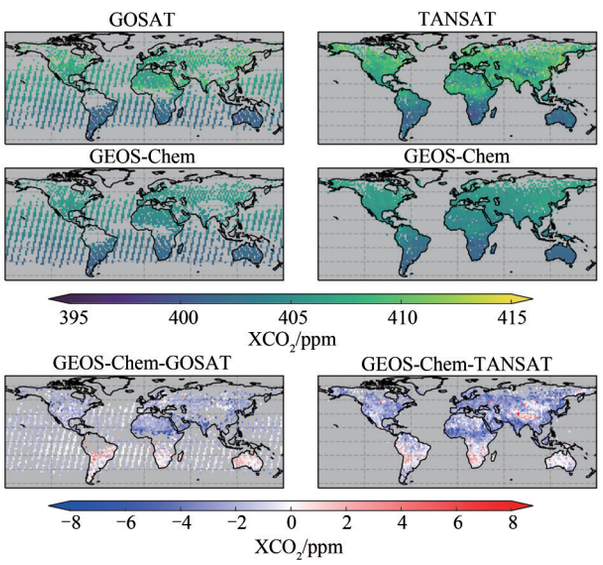

Fig. 5 GOSAT and TanSat XCO_2 for spring (MAM) 2017 and GEOS-Chem model calculations sampled according to GOSAT and TanSat, respectively. The bottom panel shows the differences between satellite and model XCO_2

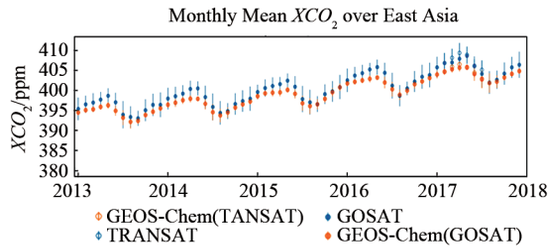

Fig.6 Time series of XCO_2 from GOSAT and GEOS-Chem model for a region around China. Also, shown is the TanSat data in 2017 and the GEOS-Chem model sampled according to TanSat

In order to analyse regions of high CO_2 emission from space-based observations such as China, we investigate XCO_2 anomalies using the method of Hakkarainen, et al. (2019). The idea is to detrend the data by removing an atmospheric background value, e.g. the hemispheric daily median, from individual observations:

$$XCO_2(\text{anomaly}) = XCO_2(\text{individual}) - XCO_2(\text{daily median})$$

In this way we can analyse the XCO_2 data over a long period of time and highlight the emission patterns. We can, for example, analyse the CO_2 data together with short-lived polluting gases (Hakkarainen, et al., 2019) or study local anthropogenic features, as done by Wang, et al. (2018) for China. Fig. 7 illustrates the northern hemispheric XCO_2 anomalies calculated for the years 2010-2016 (upper panel), and for the year 2017 (lower panel) using GOSAT data (UoL v7.2). We observe high positive XCO_2 anomalies over the main anthropogenic emission areas. Also, the emissions from biomass burning are evident in Africa and South-East Asia. Overall, the highest XCO_2 anomalies are observed in China as expected from the fossil fuel emission inventories. Due to the sparse sampling of current satellite sensors, analysing regional trends of anthropogenic emissions is challenging. One of the future goals of our ESA/MOST Dragon project is to analyse the XCO_2 anomalies also with TanSat data.

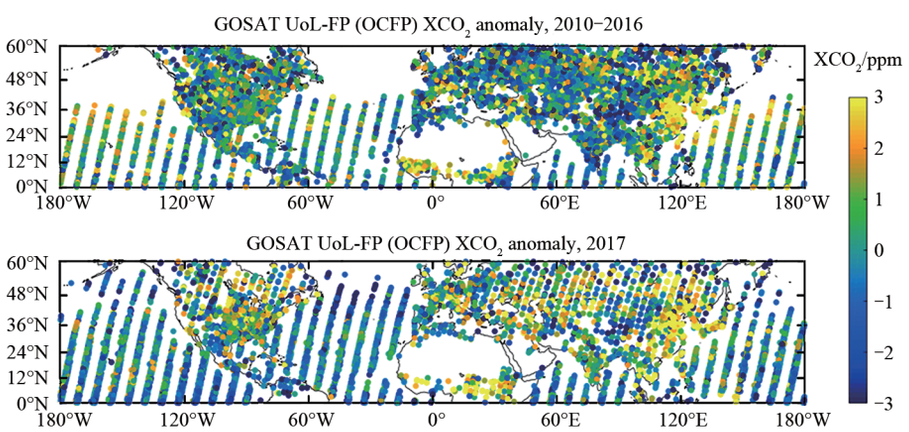

Fig.7 Northern hemispheric XCO_2 anomalies calculated for the years 2010−2016 (upper panel), and for the year 2017 (lower panel) using GOSAT UoL data product (v7.2)

5 SUMMARY

This manuscript describes the collaborative work of European (UK and Finland) and Chinese teams carried out under the framework of the Dragon programme of ESA and the Ministry of Science and Technology (MOST) towards reliable satellite observa-

tions of CO_2 over China. China is now the largest contributor to global CO_2 emissions and reliable quantification of the carbon budget is critical to advance our understanding of carbon cycle processes and to support national efforts of GHG emission reduction. To address this challenge, the National High Technology Research and Development Program of China has established the first Chinese Global Carbon Dioxide Monitoring Scientific Experimental Satellite (TanSat) which was successfully launched in December 2016.

However, the requirement on measurement precision and accuracy for space-based CO_2 observations are extremely challenging and sophisticated retrieval methods are needed together with careful validation of retrieved XCO_2. To help with the characterisation of the retrieval methods for TanSat, we have conducted the first intercomparison between two different retrieval methods (IAPCAS retrieval algorithm developed for TanSat and the University of Leicester (UoL-FP) algorithm) for TanSat for an overpass over the Lamont, USA site of the ground-based TCCON network. Results from both algorithms are in rough agreement but with a mean difference of several ppm and a clear spread between across-track pixels of TanSat. This behaviour is likely caused by uncertainties in calibration which we expect to improve in future versions of the TanSat L1b data.

To evaluate the performance of space-based CO_2 data over China and the wider region, we have compared CO_2 from GOSAT against six stations of the TCCON network in Eastern Asia. We find that observed biases and scatter in the space-based data is comparable to the global comparison even though this region is highly challenging due to its high aerosol loading. Currently only a single site is available in China which limits the ability to rigorously validate space-based data over China, but thanks to the TanSat project, activities are on-going that provide additional validation opportunities including the use of airborne AirCore systems to accurately measure vertical profiles of CO_2 up to the stratosphere. Such a system is already frequently deployed at the TCCON site at Sodankylä, Finland and via the Dragon-4 programme has now also been used for a campaign in Inner Mongolia. Eventually, such AirCore systems will be used to calibrate the TCCON instruments available in China.

To compare satellite CO_2 observations from GOSAT and TanSat against state-of-the-art model calculations, we have used calculations from the GEOS-Chem CTM. Both satellite datasets, GOSAT and TanSat, show a consistent picture when compared to the model and we find a stronger North-South gradient in the satellite dataset compared to the model. The model also shows a shallower seasonal amplitude by as much as 2 ppm when compared to the satellite observation. Finally, we have analysed anomalies in CO_2 as observed by GOSAT to demonstrates the ability of satellites to identify regions of high CO_2 emissions such as Eastern China.

Satellite observations of CO_2 can make an important contribution to our understanding of the carbon cycle in China. The first results obtained with TanSat look promising but further work on retrieval algorithms and validation is needed so that TanSat can subsequently help to provide robust information on regional CO_2 surface fluxes.

REFERENCES

Boesch, H.; Baker, D.; Connor, B.; Crisp, D.; Miller, C. Global characterization of co2 column retrievals from shortwave-infrared satellite observations of the Orbiting Carbon Observatory-2 mission. Remote Sensing 2011, 3, 270-304.

Bovensmann H.; Burrows J.P.; Buchwitz M.; Frerick J.; Noel S.; Rozanov V.V.; Chance K.V.; Goede A.P.H. SCIAMACHY: Mission objectives and measurement modes. J. Atmos. Sci., 1999, 56, 127-150.

Buchwitz M., Reuter M., Schneising O., Hewson W. , Detmers R.G., Boesch H., Hasekamp O.P., Aben I., Bovensmann H., Burrows J. P., Butz A., Chevallier F., Dils B., Frankenberg C., Heymann J., Lichtenberg G., De Mazière M., Notholt J., Parker R., Warneke T., Zehner C., Griffith D.W.T.,

Deutscher N.M., Kuze A., Suto H., Wunch D.Global satellite observations of column-averaged carbon dioxide and methane: The GHG-CCI XCO_2 and XCH_4 CRDP3 data set, *Rem*. Sens. Env., 203, 276-205, doi:10.1016/j.rse.2016.12.027, 2017a

Crisp D.; Pollock H.R.; Rosenberg R.; Chapsky L.; Lee R.A.M.; Oyafuso F.A.; Frankenberg C.; amp; apos; Dell C.W., et al. The on-orbit performance of the Orbiting Carbon Observatory-2 (OCO-2) instrument and its radiometrically calibrated products. Atmos. Meas. Tech. 2017, 10, 59-81

Chen X, Liu Y, Yang D, et al. A theoretical analysis for correcting aerosol-induced CO_2 retrieval uncertainties based on TanSat nadir observation in clear sky, *Remote Sensing*, under review.

Dirksen R. J., Sommer M., Immler F. J., Hurst D. F., Kivi R., and Vömel H.: Reference quality upper-air measurements: GRUAN data processing for the Vaisala RS92 radiosonde, *Atmos*. Meas. Tech., 7, 4463-4490, https://doi. org/10.5194/amt-7-4463-2014, 2014.

Feng, L., Palmer, P. I., Bösch, H., and Dance, S.: Estimating surface CO_2 fluxes from space-borne CO_2 dry air mole fraction observations using an ensemble Kalman Filter, *Atmos*. Chem. Phys., 9, 2619-2633, doi:10.5194/acp-9-2619-2009, 2009.

Feng L., Palmer P. I., Parker R. J., Deutscher N. M., Feist D. G., Kivi R., Morino I., and Sussmann R.: Estimates of European uptake of CO2 inferred from GOSAT X-CO2 retrievals: sensitivity to measurement bias inside and outside Europe, *Atmos*. Chem. Phys., 16, 1289-1302, doi:10.5194/acp-16-1289-2016, 2016.

Goo, T.-Y., Y.-S. Oh, VelazcoV. A.. 2017. TCCON data from Anmeyondo, South Korea, Release GGG2014R0.

TCCON data archive, hosted by CaltechDATA, California Institute of Technology, Pasadena, CA, U.S.A. https://doi.org/10.14291/tccon.ggg2014.anmeyondo01.R0/1149284

Hakkarainen, J.; Ialongo, I.; Maksyutov, S.; Crisp, D. Analysis of Four Years of Global XCO_2 Anomalies as Seen by Orbiting Carbon Observatory-2. Remote Sens. 11, 850, 2019

IPCC, 2013: Climate Change 2013: The Physical Science Basis. Contribution of Working Group I to the Fifth Assessment Report of the Intergovernmental Panel on Climate Change [Stocker, T. F., D. Qin, G. -K. Plattner, M. Tignor, S. K. Allen, J. Boschung, A. Nauels, Y. Xia, V. Bex and P.M. Midgley (eds.)]. Cambridge University Press, Cambridge, United Kingdom and New York, NY, USA, 1535 pp.

Karion A., Sweeney C., Tans P., and Newberger T.: AirCore: An Innovative Atmospheric Sampling System, J. Atmos. Ocean. Tech., 27, 1839–1853, doi:10.1175/2010jtecha1448.1, 2010.

Kivi, R. and Heikkinen, P.: Fourier transform spectrometer measurements of column CO_2 at Sodankylä, Finland, *Geosci*. Instrum. Method. Data Syst., 5, 271-279, https://doi.org/10.5194/gi-5-271-2016, 2016.

Li Z.G.; Lin C.; Li C.L.; Wang L.; Ji Z.H.; Xue H.; Wei Y.F.; Gong C. H.; Gao M.H.; Liu L., et al. Prelaunch spectral calibration of a carbon dioxide spectrometer. Measurement Science and Technology 2017, 28.

Kuze, A., Suto, H., Nakajima, M., and Hamazaki, T. (2009), Thermal and near infrared sensor for carbon observation Fourier-transform spectrometer on the Greenhouse Gases Observing Satellite for greenhouse gases monitoring, *Appl*. Opt., 48, 6716–6733, 2009

Le Quéré C., et al.Global Carbon Budget 2017, *Earth Syst*. Sci. Data, 10, 405-448, doi:10.5194/essd-10-405-2018, 2018.

Liu Y, Yang D, Cai Z. A retrieval algorithm for TanSat XCO2 observation: retrieval experiments using GOSAT data. Chin Sci Bull, 2013;58:1520–3.

Liu Y, Wang J, Yao L, et al., 2018. The TanSat mission: preliminary global observations, Science Bulletin, 63 (2018), 1200 – 1207

Liu C., Wang W., Sun Y. 2018. TCCON data from Hefei, China, Release GGG2014R0. TCCON data archive, hosted by CaltechDATA, California Institute of Technology, Pasadena, CA, U. S. A., http://dx.doi.org/10.14291/tccon.ggg2014.hefei01.R0

Morino I., MatsuzakiT., ShishimeA.. 2017. TCCON data from Tsukuba, Ibaraki, Japan, 125HR, Release GGG2014R2.

TCCON data archive, hosted by CaltechDATA, California Institute of Technology, Pasadena, CA, U.S.A. http://doi.org/10.14291/tccon.ggg2014.tsukuba02.R2

Morino I., YokozekiN., MatzuzakiT., ShishimeA.. 2017.

TCCON data from Rikubetsu, Hokkaido, Japan,Release GGG2014R2.

TCCON data archive, hosted by CaltechDATA, California Institute of Technology, Pasadena, CA, U.S.A. https://doi.org/10.14291/tccon.ggg2014.rikubetsu01.R2

Morino I., VelazcoV. A., HoriA., UchinoO., GriffithD. W. T.. 2017. TCCON data from Burgos, Philippines, Release GGG2014R0.

TCCON data archive, hosted by CaltechDATA, California Institute of Technology, Pasadena, CA, U.S.A. http://dx.doi.org/10.14291/tccon.ggg2014.burgos01.R0/1368175

Natraj, V., Boesch, H., Spurr, R. J. D., and Yung, Y. L.: Retrieval of XCO_2 from simulated Orbiting Carbon Observatory measurements using the fast-linearized R-2OS radiative transfer model, *J. Geophys*. Res., 113, D11 212, doi:10.1029/2007JD009017, 2008

Oh, Y.-S., Kenea S. T., Goo, T.-Y., Chung, K.-S., Rhee, J.-S., Ou, M.-L., Byun, Y.-H., Wennberg P. O., Kiel M., DiGangi J. P., Diskin G. S., Velazco V. A., and Griffith D. W. T.: Characteristics of greenhouse gas concentrations derived from ground-based FTS spectra at Anmyeondo, KoreaSouth, Atmos. Meas. Tech., 11, 2361-2374, https://doi.org/10.5194/amt-11-2361-2018, 2018.

Rodgers, C.D. Inverse methods for atmospheric sounding: Theory and practice. World Scientific Publishing Co. Pte. Ltd.Singapore, 2000

Shiomi K., Kawakami S., OhyamaH., AraiK., OkumuraH., TauraC., FukamachiT., SakashitaM.. 2017. TCCON data from Saga, Japan, Release GGG2014R0.

TCCON data archive, hosted by CaltechDATA, California Institute of Technology, Pasadena, CA, U.S.A. https://doi.org/10.14291/tccon.ggg2014.saga01.R0/1149283

Somkuti, P., Boesch, H., Natraj, V., Kopparla, P., Application of a PCA-Based Fast Radiative Transfer Model to XCO2 Retrievals in the Shortwave Infrared, *J. Geophys*. Res., 122(19), doi: 10.1002/2017JD027013, 2017.

Tukiainen S., RailoJ., LaineM., HakkarainenJ., KiviR., HeikkinenP., ChenH., and Tamminen (J. 2016, Retrieval of atmospheric CH_4 profiles from Fourier transform infrared data using dimension reduction and MCMC, *J. Geophys*. Res. Atmos., 121, 10,312 – 10, 327, doi:10.1002/2015JD024657.

Velazco V. A.; Morino I.; Uchino O.; Hori A.; Kiel M.; Bukosa B.; Deutscher N.M.; Sakai T.; Nagai T.; Bagtasa G.; Izumi T.; Yoshida Y.; Griffith D. W. T. TCCON Philippines: First Measurement Results, Satellite Data and Model Comparisons in Southeast Asia, Remote Sens. 2017, 9, 1228.

Wang Z., Warneke T., Deutscher N. M., Notholt J., Karstens U., Saunois M., Schneider M., Sussmann R., Sembhi H., Griffith D. W. T., Pollard D. F., Kivi R., Petri C., Velazco V. A., Ramonet M., and Chen H.: Contributions of the troposphere and stratosphere to CH_4 model biases, *Atmos*. Chem. Phys., 17, 13283-13295, https://doi.org/10.5194/acp-17-13283-2017, 2017.

Wunch, D., et al., A method for evaluating bias in global measurements of CO_2 total columns from space, *Atmos*. Chem. Phys., 11, 12317-12337, doi:10.5194/acp-11-12317-2011, 2011.

Yang DX, Zhang HF, Liu Y, et al. Monitoring carbon dioxide from space: retrieval algorithm and flux inversion based on GOSAT data and using CarbonTracker-China, Adv Atmos Sci, 2017;34:965 – 76.

Yang DX, Liu Y, Cai ZN, et al. An advanced carbon dioxide retrieval algorithm for satellite measurements and its application to GOSAT observations. Sci Bull, 2015;60:2063 – 6.

Yang D, Liu Y, Cai Z, et al., 2018: First Global Carbon Dioxide Maps Produced from TanSat Measurements, *Adv.* Atmos. Sci., 35(6), 1 – 4

Zhang J.Q.; Shao J.B.; Yan C.X. Cloud and aerosol polarimetric imager. In Selected papers from conferences of the photoelectronic technology committee of the chinese society of astronautics: Optical imaging, remote sensing, and laser-matter interaction 2013,

Ojeda Castaneda J.; Han S.; Jia P.; Fang J.; Fan D.; Qian L.; Gu Y.; Yan X., Eds. 2014; Vol. 9142.